Binary mixtures of magnetic fluids

W. Fenz and R. Folk
Institute for Theoretical Physics, Linz University, A-4040 Linz, Austria
(Received 17 October 2002; published 27 February 2003)

We study a binary mixture of a van der Waals fluid and a ferromagnetic fluid at zero magnetic field on the basis of the mean field Ising fluid model and the van der Waals theory with quadratic mixing rules. Depending on three reduced parameters, the phase diagram shows a surface of magnetic phase transitions and lines of tricritical points, critical end points, and magnetic consolute points. First-order phase transition surfaces and critical lines are calculated numerically. For the line of tricritical points, which can occur in two different topologies, an analytic expression is derived. All higher-order lines and coexistence surfaces are visualized in three-dimensional x, T, p and ξ, T, p diagrams, where ξ is a mapping of Δ, the conjugated field of the mole fraction x, on the unit interval.

DOI: 10.1103/PhysRevE.67.021507 PACS number(s): 05.70.Fh, 82.60.Lf, 64.60.−i, 64.60.Kw

I. INTRODUCTION

The investigation of the global phase behavior of binary mixtures began with the work of van Konynenburg and Scott in 1980 [1], in which they calculated phase equilibria and critical lines of van der Waals mixtures, and classified five distinct types (denoted as I–V) of phase diagrams, each corresponding to a certain region in the space of the two mixture parameters. Later, more types were discovered by using other theories such as the Ree equation of state [2], the simplified-perturbed-hard-chain theory (SPHCT) [3,4], the lattice gas model [5–8], the Redlich-Kwong equation of state [9], and the Carnahan-Starling-Redlich-Kwong equation of state [10]. Only systems that lie on the boundaries between the regions of the global phase diagram can exhibit multicritical points, e.g., symmetrical tricritical points [11,12] or a van Laar point [13].

In this paper, we deal with mixtures with one component being a magnetic fluid. This enlarges the thermodynamic space, and contrary to nonmagnetic binary mixtures multicritical phase transitions become a common phenomenon under certain *thermodynamic conditions*, not only under very specific conditions for the interaction parameters in *global space*.

As an example for such a system one might consider He^3-He^4 mixtures at low temperatures. This quantum liquid becomes superfluid along the concentration and pressure dependent λ line of second-order phase transitions. This phase transition can be represented by the XY model for planar magnets. At a certain concentration a tricritical point exists and demixing sets in into a superfluid (=magnetic) He^4 rich phase and a normal liquid He^3 rich phase [14]. At higher temperature a concentration dependent line of plait points is present.

Following Hemmer and Imbro [15], we use as a simple one-dimensional model for a magnetic fluid the van der Waals equation with an additional term including the square of the magnetization m and the strength of the magnetic interaction a_m, together with the mean field equation of state of an Ising system. Such an Ising fluid undergoes liquid-vapor as well as paramagnetic-ferromagnetic phase transitions, and depending on the ratio R_m of the magnetic and nonmagnetic interaction parameters a_m and a, it can have three topologically different types of phase diagrams, two of which show a tricritical point. We would like to mention that Ising fluids may be mapped to symmetrical binary mixtures [11]. In this way our mixture of an Ising fluid and a van der Waals fluid may also be applicable to ternary mixtures.

The questions we wanted to address were if and for which parameters the mixture of an Ising and a van der Waals fluid exhibits a line of tricritical points, and what is the minimal mole fraction of the Ising fluid component necessary for the mixture to show tricriticality. Another topic of interest was whether critical lines with finite magnetization can occur, which would be tantamount to the coexistence of two magnetic phases in the mixture. In pure magnetic fluids, such order-order critical points have been found in mean field and modified mean field calculations of Heisenberg fluids, but only for negative values of R_m [16,17]. We also restrict ourselves to fluid phases since otherwise the phase diagrams would be rather complicated. Solid phases within mean field theory have been considered for classical Heisenberg fluids in Ref. [18], extending the approach of [15].

The paper is organized as follows: After defining the model free energy and the condition of phase equilibria, we derive the equations to be solved for critical points, magnetic critical points, and tricritical points. Combining the results of all these we are able to present the topology of the overall phase diagram for different sets of model parameters. Concluding with a short discussion we comment in Appendix A on the representation of the phase diagrams and in the following appendixes we explain in more detail the calculation of critical and tricritical lines and phase equilibria.

II. MODEL

Let us consider a binary mixture in the molar volume V consisting of a van der Waals fluid (fluid 1) and an Ising fluid (fluid 2). The mole fraction of the second component shall be denoted as x and its magnetization per particle as m. The total magnetization per particle is accordingly $m_{tot}=xm$. We describe our system with a van der Waals like equation of state,

$$p(T,V,x,m)=\frac{RT}{V-b}-\frac{a(x,m)}{V^2}, \tag{1}$$

where the attraction parameter a contains the nonmagnetic attraction according to the quadratic mixing rule and the magnetic interaction of one component

$$a(x,m)=a_{11}(1-x)^2+2a_{12}x(1-x)+\left(a_{22}+\frac{1}{2}a_m m^2\right)x^2, \tag{2}$$

and the size parameter b is assumed constant. In Eq. (2), a_{11} and a_{22} denote the nonmagnetic interactions between particles of the same kind, a_{12} the nonmagnetic interaction between unlike particles, and a_m the magnetic interaction in the Ising fluid. The factor 1/2 was chosen in order to be consistent with Ref. [15] for the case of the pure ideal Ising fluid. For the magnetization, the equation of state at zero magnetic field reads

$$m=\tanh\left(\frac{a_m x m}{VRT}\right). \tag{3}$$

The corresponding molar Helmholtz free energy of the system described by Eqs. (1) and (3) with respect to the reference state of an ideal unmixed gas with molar volume $V^0=b$ is given by

$$\begin{aligned}A^{rel}(T,V,x,m)=A(T,V,x,m)-A^0(T,V^0)=xA_s(T,m)\\ +RT[(1-x)\ln(1-x)+x\ln x]\\ -RT\ln\left(\frac{V-b}{b}\right)-\frac{a(x,m)}{V},\end{aligned} \tag{4}$$

where

$$A_s(T,m)=RT\left(\frac{1-m}{2}\ln\frac{1-m}{2}+\frac{1+m}{2}\ln\frac{1+m}{2}\right) \tag{5}$$

is the entropy part of the free energy of the Ising fluid component. Following van Konynenburg and Scott [1], we define the reduced parameters ζ and Λ describing the nonmagnetic interactions in the mixture as

$$\zeta=\frac{a_{22}-a_{11}}{a_{11}+a_{22}}, \tag{6}$$

$$\Lambda=\frac{a_{11}-2a_{12}+a_{22}}{a_{11}+a_{22}}. \tag{7}$$

In our case, however, a third parameter is needed to fully characterize the system, which is

$$R_m=\frac{1}{2}\frac{a_m}{a_{22}}, \tag{8}$$

denominating the ratio of magnetic and nonmagnetic interaction in the magnetic fluid component. For convenience, we introduce reduced variables by scaling the variables by parameters of component 2 (normalizing the critical temperature and pressure in absence of the magnetic interaction to 1),

$$T_r=\frac{27}{8}\frac{bRT}{a_{22}}=\frac{27}{4}R_m\frac{bRT}{a_m}, \tag{9}$$

$$p_r=\frac{27b^2p}{a_{22}}, \tag{10}$$

$$V_r=\frac{V}{b}. \tag{11}$$

III. PHASE EQUILIBRIA

As a condition for the coexistence of two phases α and β, characterized by V_α, x_α, m_α and V_β, x_β, m_β, at a temperature T_0 and pressure p_0 we take the equality of the chemical potentials of the two components μ_1 and μ_2 in both phases:

$$\mu_1(T_0,V_\alpha,x_\alpha)=\mu_1(T_0,V_\beta,x_\beta), \tag{12}$$

$$\mu_2(T_0,V_\alpha,x_\alpha,m_\alpha)=\mu_2(T_0,V_\beta,x_\beta,m_\beta), \tag{13}$$

where the chemical potentials are derived from the Helmholtz free energy (4) as

$$\mu_1^{rel}=-\frac{2[a_{11}(1-x)+a_{12}x]}{V}+RT\ln\left(b\frac{1-x}{V-b}\right)+RT\frac{V}{V-b}, \tag{14}$$

$$\begin{aligned}\mu_2^{rel}=-\frac{2\left[\left(a_{22}+\frac{1}{2}a_m m^2\right)x+a_{12}(1-x)\right]}{V}+A_s(T,m)\\ +RT\ln\frac{bx}{V-b}+RT\frac{V}{V-b}.\end{aligned} \tag{15}$$

In addition to conditions (12) and (13), the two phases must obey the thermodynamic and magnetic equations of state (1) and (3) at T_0 and p_0,

$$p(T_0,V_i,x_i,m_i)=p_0, \tag{16}$$

$$m_i=\tanh\left(\frac{a_m x_i m_i}{V_i RT_0}\right), \tag{17}$$

where $i=\alpha$, β. By solving the six equations (12), (13), (16), and (17) for the six variables characterizing the coexisting phases, one can find the first-order phase transition surfaces in x, T, p space.

IV. CRITICAL LINES

In order to locate the critical points, plait points as well as consolute points, in the magnetic mixture, we consider the magnetic degrees of freedom as eliminated by the magnetic equation of state. Thus we can follow the procedure used in a nonmagnetic binary fluid mixture. There the critical point

is characterized by the onset of concavity in the Gibbs free energy per mol G as a function of the mole fraction x:

$$\left(\frac{\partial^2 G}{\partial x^2}\right)_{T,p,m}=0, \tag{18}$$

$$\left(\frac{\partial^3 G}{\partial x^3}\right)_{T,p,m}=0. \tag{19}$$

Expressing these conditions in terms of the Helmholtz free energy yields

$$A_{2V}A_{2x}-A_{Vx}^2=0, \tag{20}$$

$$A_{3V}A_{2x}^2-3A_{2Vx}A_{Vx}A_{2x}+3A_{V2x}A_{Vx}^2-A_{3x}A_{2V}A_{Vx}=0, \tag{21}$$

$$A_{3x}A_{2V}^2-3A_{2xV}A_{Vx}A_{2V}+3A_{x2V}A_{Vx}^2-A_{3V}A_{2x}A_{Vx}=0, \tag{22}$$

where

$$A_{iVjx}\equiv\left(\frac{\partial^{i+j}A}{\partial^i V\partial^j x}\right)_{T,m}. \tag{23}$$

Note that Eq. (22) is not independent of the others. For zero magnetization, equations (20)–(22) describe the critical points in a conventional binary mixture. In that case, it is possible to eliminate the temperature and combine the three equations to a single equation involving only powers of x and V [1].

In order to find critical points with nonzero magnetization, according to our philosophy, one has to take into account that the magnetic equation of state (3) induces an additional implicit dependency of the Helmholtz free energy on volume and concentration,

$$A=A[V,x,m(V,x)], \tag{24}$$

making the derivatives in Eqs. (20)–(22) a lot more complicated. In the resulting equations, T cannot be eliminated anymore and thus a system with four unknown variables T, V, x, and m consisting of Eqs. (20), (21) and the equations of state (1) and (3) has to be solved to locate a magnetic critical point at a certain pressure. The full equations are given in Appendix B. We checked the location of the critical lines by comparing with the results when calculating the phase equilibria for different pressures. In this way we avoided the calculation of the next higher order of free energy derivatives.

V. SURFACE OF MAGNETIC PHASE TRANSITIONS

In zero magnetic field a liquid and also a binary mixture may order magnetically like a solid even for short range magnetic interaction. This has been demonstrated recently in the liquid alloy $Co_{80}Pd_{20}$ [19,20]; however, this fluid is represented by a Heisenberg fluid rather than an Ising fluid. Evidence of a magnetic transition has been given also by computer simulations [16,21–23]. We consider the locus of points where a second-order phase transition from ferromagnetic to paramagnetic state occurs in mean field order. From Eq. (3) one can see that this happens for

$$V=\frac{xa_m}{RT}, \quad V_r=\frac{27}{4}\frac{xR_m}{T_r}. \tag{25}$$

Equation (25) defines a surface in x, T, V space. Via the equation of state (1), it transforms to a surface in x, T, p space whose shape depends on the three mixture parameters:

$$p_r(T_r,x)=16T_r^2\left(\frac{1}{27R_m x-4T_r}-\frac{1}{27R_m^2x^2}\frac{a(x,0)}{a_{22}}\right). \tag{26}$$

There is for each concentration and pressure a magnetic phase transition with T_c going to zero in the limiting case when the concentration of the magnetic liquid goes to zero since V stays finite ($V>b$). Contrary to what is known from the solid magnetic solutions there is no percolation limit at finite concentrations [24], so that this feature is not an artifact of the mean field approximation.

Equation (26) defines the surface of second-order magnetic phase transitions, but it might be unstable for certain values. There are two possibilities: (i) the surface becomes unstable in a line of tricritical points, and/or (ii) it intersects another first-order phase transition surface in a line of critical end points. In the first case the line of tricritical points is the border line to the surface of first-order magnetic or liquid phase transitions. Examples for both scenarios are presented in the following sections.

VI. TRICRITICAL LINE

The pure Ising fluid shows a tricritical point for values of $R_m\gtrsim 0.211$. In order to find a tricritical point in the van der Waals-Ising fluid mixture one would, in principle, have to solve the equation

$$\left(\frac{\partial^4 G}{\partial x^4}\right)_{T,p,m}=0 \tag{27}$$

together with Eqs. (18) and (19). One can, however, make use of the fact that at the tricritical point the density and concentration differences go to zero and the phase transition becomes second order. Hence a tricritical point can be regarded as a critical point in the limit of zero magnetization in the ferromagnetic phase, or as a critical point on the surface of magnetic phase transitions. In order to take the limit $m\to 0$ in Eq. (20) it is necessary to replace m^2 with the expansion of Eq. (3) for small m,

$$m^2\sim 3\left(1-\frac{VRT}{xa_m}\right)=3\left(1-\frac{4V_rT_r}{27xR_m}\right), \tag{28}$$

and let the volume V approach the critical value given in Eq. (25). Since the only variables left in Eq. (20) are then x and T, one can find the tricritical temperature T^t for arbitrary

concentrations x without making use of Eqs. (21) and (22). The explicit expression for T^t as a function of x is

$$T_r^t(x)=\frac{27R_m}{4}\left(x-\sqrt{\frac{x^3}{A(x)-\dfrac{B^2(x)}{C-\dfrac{1}{1-x}}}}\right), \quad (29)$$

where

$$A(x)=2\frac{a(x,0)}{a_m}+\frac{3}{2}x^2, \quad (30)$$

$$B(x)=\frac{1}{2}\frac{dA(x)}{dx}, \quad (31)$$

$$C=\frac{dB(x)}{dx}. \quad (32)$$

Equation (29) inserted into the equation of the magnetic phase transition surface (26) defines a line of tricritical points in x, T_r, p_r space.

Physical conditions define the range of existence of this line, namely, a real and positive value for the temperature and a positive value for the pressure for concentration values between zero and one. Moreover, the tricritical line might cross other phase transition surfaces ending in a tricritical end point.

Formally the tricritical line starts in the phase diagram at $x=1$ (apart from values of R_m where instead of a tricritical point a critical end point is present) at a temperature [15]

$$T_r^t(1)=\frac{27R_m}{4}\left[1-\left(\frac{3}{2}+\frac{1}{R_m}\right)^{-1/2}\right], \quad (33)$$

the tricritical temperature of the pure Ising fluid. On the other side at $x=0$, which corresponds to the pure van der Waals fluid, there is no tricritical point. Therefore the line of tricritical points must go into a direction perpendicular to the concentration at some nonzero value of x or at least become unstable somewhere between $x=1$ and $x=0$. Let us have a look at the behavior of the tricritical line in the limit $V\rightarrow b$. Then there are three possibilities: (i) for a finite tricritical temperature and finite concentration the pressure goes to infinity according to Eqs. (1) and (25), (ii) for $x=0$ and $T_r^t=0$ the pressure reaches a finite positive value, or (iii) for a finite concentration and finite tricritical temperature the pressure goes to zero.

Equation (25) tells us that if $V\rightarrow b$, the surface of magnetic phase transitions approaches the plane defined by

$$x=\frac{bRT}{a_m}, \quad x=\frac{4T_r}{27R_m}. \quad (34)$$

Comparing this with Eq. (29), we see that the tricritical point lies on that plane if the expression in the square root vanishes. This happens for $x\neq 0$ if x takes on the value

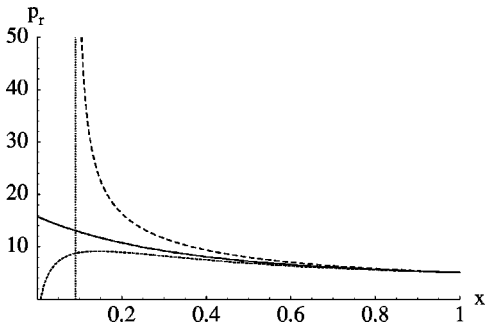

FIG. 1. Projection of the tricritical line on the x, p_r plane for systems with $\zeta=0.5$; $R_m=0.5$; and $\Lambda=-0.15$ ($x_\infty^t=0.091$; long-dashed line), $\Lambda=-0.1875$ ($x_\infty^t=0$; solid line), and $\Lambda=-0.21$ ($x_\infty^t=-0.064$; short-dashed line).

$$x_\infty^t=\frac{4\,\Lambda+R_m(1+\zeta)}{4\,\Lambda+3\,R_m(1+\zeta)} \quad (35)$$

and $T_{r\infty}^t$ is given by Eq. (34) inserting x_∞^t. Thus if $0<x_\infty^t<1$ we have case (i), and the tricritical line escapes to infinity at these finite values for temperature and concentration. This behavior is quite similar to the behavior of a demixing line in a nonmagnetic mixture in the corresponding classes [1,25,26]. For $0<x<x_\infty^t$, there will be no tricritical point since the square root in Eq. (29) will become complex (see Fig. 1, long-dashed line).

If $x_\infty^t\leqslant 0$ or $x_\infty^t>1$, however, the tricritical pressure will remain finite for $x\in[0,1]$, and we have to consider case (ii) or (iii). Now at $x=0$ one always finds a tricritical pressure of

$$p_r^t(x=0)=\lim_{x\rightarrow 0}p_r^m[T_r^t(x),x]=-27\frac{1-\zeta}{1+\zeta}, \quad (36)$$

which is negative since $\zeta\in\,]-1,1[$. This means that the tricritical pressure changes its sign at some $0<x_0<1$ and the tricritical line becomes unstable [case (iii), see Fig. 1, short-dashed line].

The only exception to Eq. (36) occurs for parameter values where x_∞^t is exactly zero, in which case

$$p_r^t(x=0)=-27\frac{1-3\zeta+2\Lambda}{1+\zeta}. \quad (37)$$

The value of this pressure can be positive for a suitable choice of the parameters Λ and ζ. Still, however, according to Eq. (29), the tricritical temperature for $x=0$ is zero, and thus there is also in this case no tricritical point with finite temperature in the pure van der Waals fluid [case (ii), see Fig. 1, solid line]. In the last two cases the tricritical line becomes unstable and ends in a *tricritical end point* on a first-order coexistence surface (see one example of such a case below).

The set of parameters Λ, ζ, R_m for which x_∞^t is zero, form a boundary in the three-dimensional global phase space that separates two distinct types of phase diagrams, one with a line of tricritical consolute points and one with a line of tricritical plait points. This surface, defined by the equation

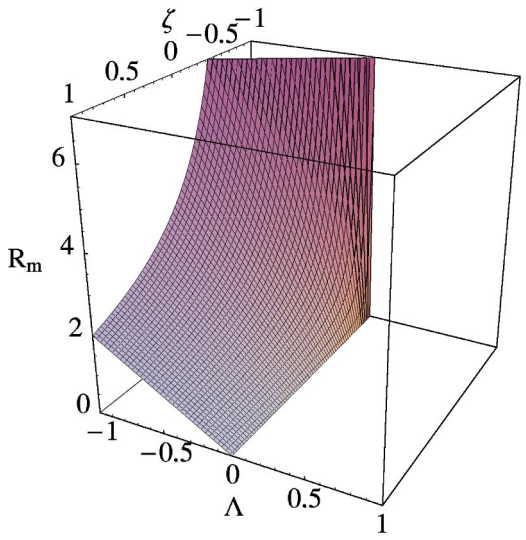

FIG. 2. Plot of the boundary surface in ζ, Λ, R_m space separating the two types of behavior of the tricritical line. For parameter values above the surface, the tricritical line has the character of a consolute line.

$$\Lambda = -\frac{R_m}{4}(1+\zeta), \tag{38}$$

is shown in Fig. 2.

VII. DIFFERENT TOPOLOGIES OF PHASE DIAGRAMS

We now present phase diagrams for special values of the model parameters. The idea behind the three-dimensional figures is explained in Appendix A. We selected out of the rich variety cases where different types of tricritical lines appear.

A. Mixture with ideal Ising fluid

First we consider a mixture of a van der Waals fluid and an ideal Ising fluid with pure magnetic interaction, i.e., $a_{22}=0$ and $a_{12}=0$, respectively, $\zeta=-1$, $\Lambda=1$, and $R_m=\infty$. In this case only the ratio $r\equiv a_{11}/a_m$ can vary. Of course, the reduced variables (9) and (10) cannot be used for such a system, instead we take for the reduced temperature and the reduced pressure

$$T_r=\frac{bRT}{a_m}, \quad p_r=\frac{b^2p}{a_m}. \tag{39}$$

For these parameters, the magnetic surface is simply given by $V_r=x/T_r$ and the limiting value of the concentration and temperature on the tricritical line in Eq. (35) becomes

$$x^t_\infty=\frac{1+4r}{3+4r}, \quad T^t_{r\infty}=\frac{1+4r}{3+4r}, \tag{40}$$

which lies between 1/3 and 1, corresponding to the limiting cases of vanishing attractive interaction in the van der Waals fluid and the ideal Ising fluid, respectively. Hence, the tricritical line starts at the tricritical point of the ideal Ising fluid and approaches infinite pressure at $x=x^t_\infty$ and $T=T^t_{r\infty}$. The character of the tricritical line crosses over from a gas liquid critical point for the pure ideal Ising fluid to a demixing critical point in the mixture. Below the tricritical temperature, the mixture forms two phases, a paramagnetic phase with a low concentration and a ferromagnetic phase with a higher concentration of the ideal Ising fluid. Note, however, that in the whole crossover regime the densities of the two phases below the tricritical temperature are also different. From the critical point in the pure van der Waals fluid a critical line originates, which also takes on the character of a consolute line in the mixture but ends on the coexistence surface of paramagnetic and ferromagnetic phases in a critical end point. From there, a three-phase line (line of triple points) continues to zero pressure and temperature.

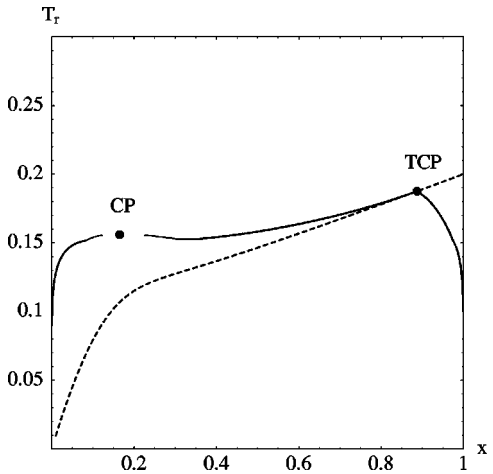

FIG. 3. x, T_r diagram of a mixture with $\zeta=-1$, $\Lambda=1$, $R_m=\infty$, and $r=0.5$ at $p_r=0.05$. CP, critical point; TCP, tricritical point; full lines, first-order phase transitions; dashed line, magnetic phase transitions.

Figures 3 and 4 are x, T_r diagrams of a mixture with $r=0.5$, $x^t_\infty=T^t_{r\infty}=0.6$ at different pressures showing the phase coexistence curves, critical and tricritical points, and the line

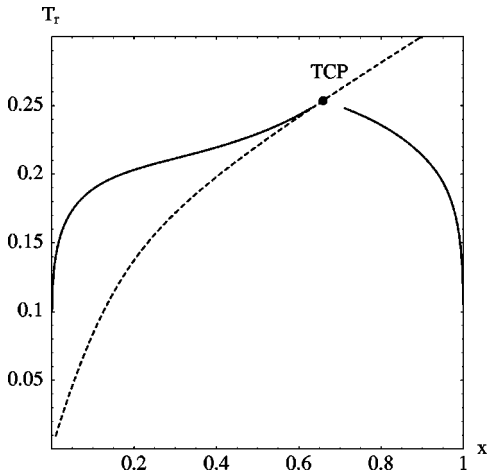

FIG. 4. x, T_r diagram of a mixture with $\zeta=-1$, $\Lambda=1$, $R_m=\infty$, and $r=0.5$ at $p_r=0.15$. TCP, tricritical point; full lines, first-order phase transitions; dashed line, magnetic phase transitions.

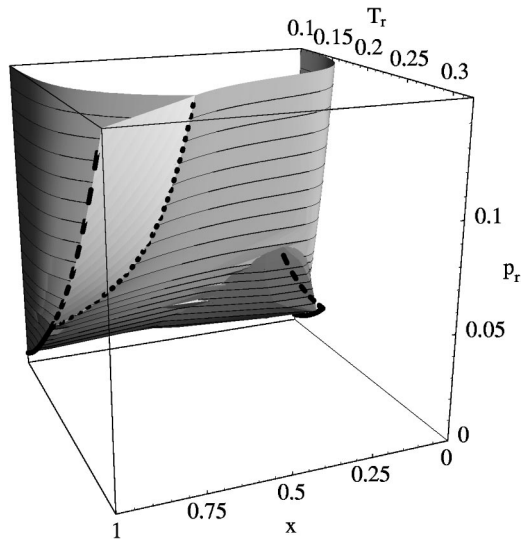

FIG. 5. x, T_r, p_r diagram of a mixture with $\zeta=-1$, $\Lambda=1$, $R_m=\infty$, and $r=0.5$. Thick lines, liquid-vapor curves of the pure substances; thin lines, isobaric curves on the first-order surface; dotted line, tricritical line; dashed lines, critical lines.

of magnetic phase transitions. At $p_r=0.05$ one can see two consolute points, a critical and a tricritical one, while at $p_r=0.15$, well above the pressure of the critical end point, only the tricritical consolute point is left. These diagrams are cross sections of the whole phase diagram (see Fig. 5) in x, T_r, p_r space including the surface of magnetic phase transitions (light gray) and the phase coexistence surfaces (dark gray). The liquid phase coexistence surfaces penetrate each other defining coexistence of three phases. In Fig. 6, we have replaced the variable x by its conjugated field variable $\Delta=\mu_1-\mu_2$. Since Δ takes on all values from $-\infty$ to $+\infty$, as x varies between 0 and 1, we did not use Δ itself as a coordinate in the phase diagram, but rather

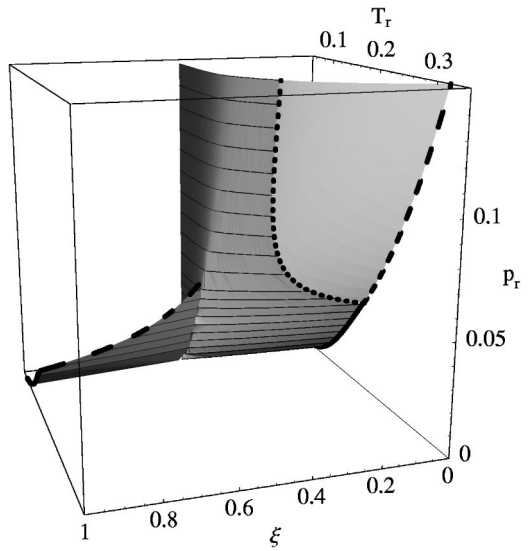

FIG. 6. ξ, T_r, p_r diagram of a mixture with $\zeta=-1$, $\Lambda=1$, $R_m=\infty$, and $r=0.5$. Thick lines, liquid-vapor curves of the pure substances; thin lines, isobaric curves on the first-order surface; dotted line, tricritical line; dashed lines, critical lines.

$$\xi \equiv \frac{1}{1+e^{-\Delta/RT}}, \tag{41}$$

which lies between 0 and 1 for Δ between $-\infty$ and $+\infty$. $\xi=0$ corresponds to the pure component 2 ($x=1$), $\xi=1$ to the pure component 1 ($x=0$). In a ξ, T_r, p_r diagram, the phase coexistence surfaces, which enclose the two-phase volume in the x, T_r, p_r diagram, form interfaces between the coexisting phases, since ξ is continuous at a first-order phase transition. The two coexistence surfaces (dark gray), one with a jump in magnetization and one separating two nonmagnetic phases, are bounded by the liquid-vapor curves, the critical line, and the tricritical line and meet along a line of triple points. At the tricritical line the paramagnetic-ferromagnetic phase transition becomes second order, and the coexistence surface passes into the surface of magnetic phase transitions (light gray).

B. General case

In the general case there are many possibilities for different topologies of the phase diagram depending on the strength of the magnetic interaction parameter. For the Ising fluid three different types of phase diagrams have been found [15] for increasing R_m: (i) without a tricritical point but a critical end point and a gas liquid critical point; (ii) with a critical end point, a tricritical point, and a gas liquid critical point; and (iii) with a tricritical point only (like the ideal Ising fluid). The nonmagnetic parameters, on the other hand, define five different classes found by van Konynenburg and Scott [1]. We consider a van der Vaals mixture of type I in their classification. This class constitutes the most simple topology and is characterized by a line of plait points (gas liquid critical points) connecting the pure fluids, no demixing transition appears. In the following we discuss three different topologies showing tricritical lines and the appearance of a critical line in the magnetic phase.

We are interested in the effect of adding a magnetic interaction to one component of the mixture. At saturation, $m=1$, we recover a binary mixture with changed parameters Λ and ζ, shifting the mixture to type III (containing a line of consolute points). Thus we expect interesting effects in zero magnetic field induced by the magnetic interaction and the existence of a ferromagnetic phase.

1. Tricritical consolute point line and plait point line

We choose the parameters $\zeta=0.5$ and $\Lambda=-0.05$ and add a weak magnetic interaction to the second component with the ratio $R_m=0.2$. Although there is no tricritical point in the pure Ising fluid for this value of R_m, the phase diagram shows a tricritical line starting at a certain concentration in a *tricritical end point* on the first-order surface of liquid-vapor phase transitions. As p_r goes to infinity, the tricritical line reaches the limiting concentration $x^t_\infty=0.1429$ and the tricritical temperature $T^t_{r\infty}=0.1929$. Such a topology is quite similar to He^3-He^4 mixtures, with differences for low concentrations.

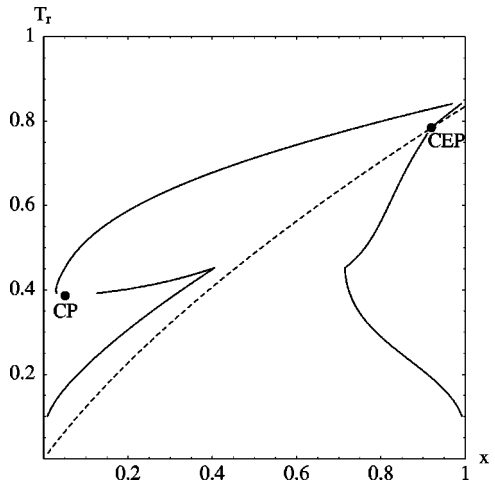

FIG. 7. x, T_r diagram of a mixture with $\zeta=0.5$, $\Lambda=-0.05$, and $R_m=0.2$ at $p_r=0.5$. CP, critical point; CEP, critical end point; full lines, first-order phase transitions; dashed line, magnetic phase transitions.

Figures 7–9 are examples of x, T_r diagrams at increasing pressures. Starting from the situation where only one critical point and a triple point are present, Fig. 7, a tricritical point appears in addition to the critical point and the triple point disappeared (Fig. 8). Increasing the pressure further one finds a situation where a tricritical point and two different critical points exist (not shown) and finally for pressures large enough only the tricritical point remains (see Fig. 9). These cross sections should be compared with Fig. 10 where the whole phase diagram in x, T_r, p_r space is shown. Again the phase diagram in field space, ξ, T_r, p_r, (see Fig. 11) shows two transition surfaces: the first-order gas-liquid phase transition surface (dark gray in front) ending in a line of plait points and the surface of magnetic phase transitions consisting of a second-order part (light gray) and a first-order part corresponding to liquid-liquid transitions (dark gray) separated by the tricritical line. These surfaces intersect along a triple line (the dark ones) and along a line of critical end points (the light gray and the dark one in front). These two lines and the tricritical line meet in the tricritical end point (in the figure this is occluded by the gas-liquid surface in front).

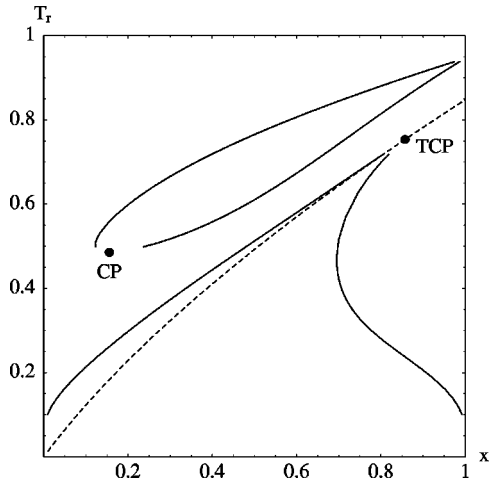

FIG. 8. x, T_r diagram of a mixture with $\zeta=0.5$, $\Lambda=-0.05$, and $R_m=0.2$ at $p_r=0.8$. CP, critical point; TCP, tricritical point; full lines, first-order phase transitions; dashed line, magnetic phase transitions.

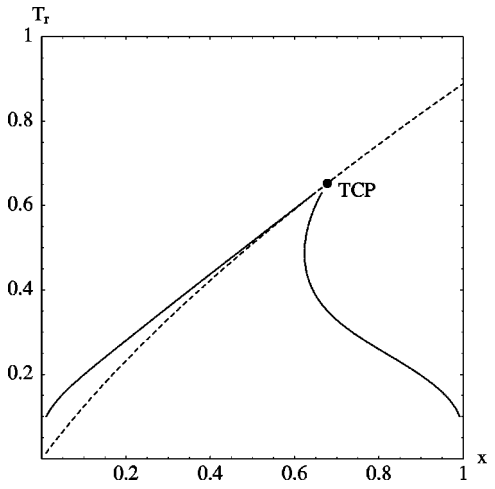

FIG. 9. x, T_r diagram of a mixture with $\zeta=0.5$, $\Lambda=-0.05$, and $R_m=0.2$ at $p_r=2$. TCP, tricritical point; full lines, first-order phase transitions; dashed line, magnetic phase transitions.

2. Consolute point line within the magnetic phase and tricritical plait point line

In order to present an example where the tricritical line remains below a finite value of pressure we choose the parameter values $\zeta=0.5$, $\Lambda=-0.25$, and $R_m=0.5$. In this case the value of x_∞^t is negative, namely, $x_\infty^t=-0.2$. From the x, T_r, p_r diagram (Fig. 12) we can see that there is no tricritical point at high pressures, but instead a line of consolute points *within* the magnetically ordered phase (we call such a point

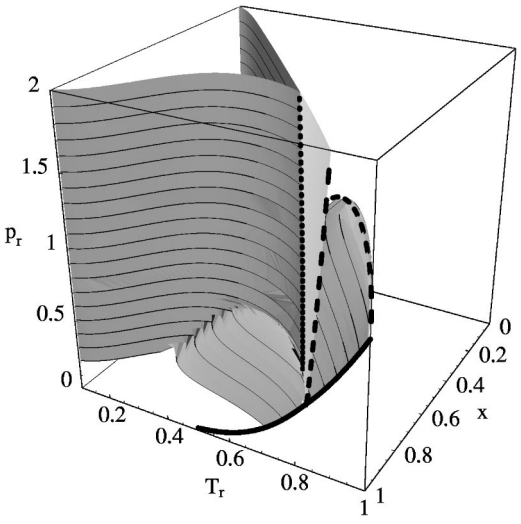

FIG. 10. x, T_r, p_r diagram of a mixture with $\zeta=0.5$, $\Lambda=-0.05$, and $R_m=0.2$. Thick line, liquid-vapor curve of the pure Ising fluid; thin lines, isobaric curves on the first-order surface; dotted line, tricritical line; dashed lines, critical lines.

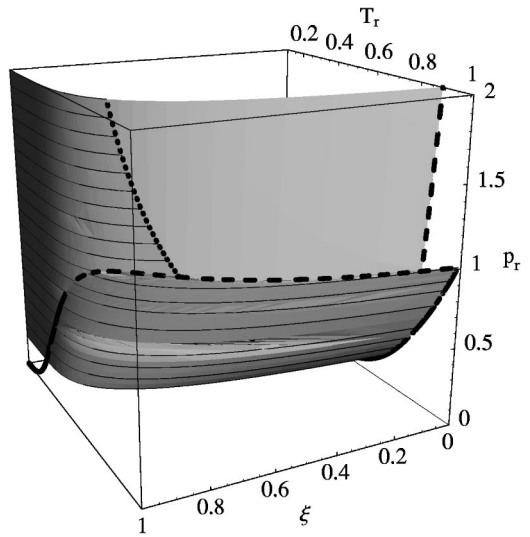

FIG. 11. ξ, T_r, p_r diagram of a mixture with $\zeta=0.5$, $\Lambda=-0.05$, and $R_m=0.2$. Thick lines, liquid-vapor curves of the pure substances; thin lines, isobaric curves on the first-order surface; dotted line, tricritical line; dashed lines, critical lines.

magnetic consolute point) continues till infinite pressure, approaching $x_\infty=0.499$ and $T_{r\infty}=0.2814$. Thus demixing is induced by the magnetic interaction and the finite magnetization of the mixture. Both phases in which the decomposition takes place are magnetically ordered.

The x, T_r diagram again shows immiscibility at low temperatures (Fig. 13), a tricritical point (Fig. 14), and in a narrow pressure range two tricritical points and a magnetic consolute point (Fig. 15). Above a maximum tricritical pressure $p^t_{max}=6.9847$, only the magnetic consolute point remains. The magnetic phase transition line ends on the coexistence curve in a critical end point.

The ξ, T_r, p_r-phase diagram (Fig. 16) summarizes again in a compact way the whole variety of phase lines and surfaces present in this topology. The first-order gas liquid surface (in front) ending in a *line of tricritical plait points* continues as a first-order demixing surface, bounded by a *line of magnetic consolute points*, at higher pressures. The magnetic phase transition surface intersects this demixing surface along a line of critical end points at values of ξ near 1. This line meets the tricritical line in a tricritical end point, which is connected by a short line of triple points to the magnetic critical end point, where the line of magnetic consolute points hits the surface of first-order phase transitions. These features are not visible in Fig. 16 but in Fig. 17 they are illustrated schematically.

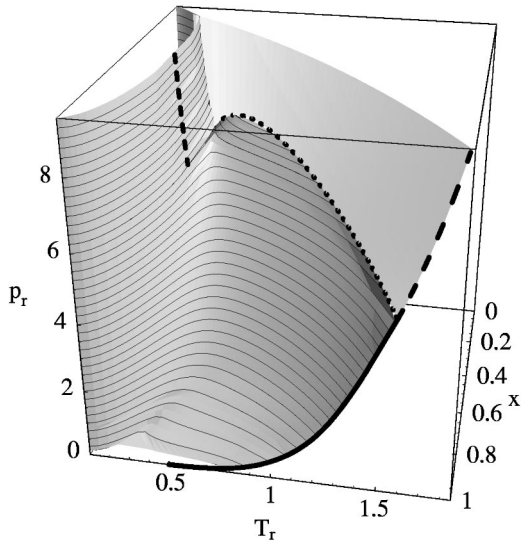

FIG. 12. x, T_r, p_r diagram of a mixture with $\zeta=0.5$, $\Lambda=-0.25$, and $R_m=0.5$. Thick lines, liquid-vapor curves of the pure substances; thin lines, isobaric curves on the first-order surface; dotted line, tricritical line; dashed lines, critical lines.

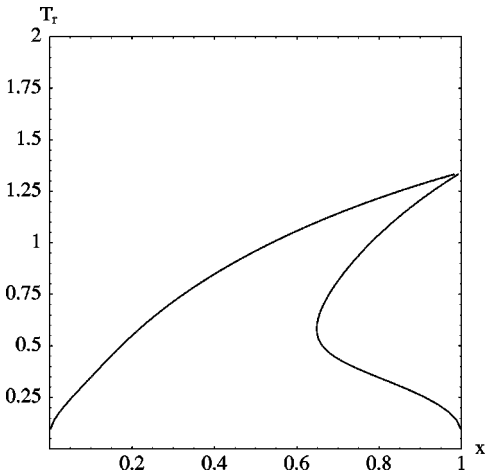

FIG. 13. x, T_r diagram of a mixture with $\zeta=0.5$, $\Lambda=-0.25$, and $R_m=0.5$ at $p_r=2.5$. Full lines, first-order phase transitions.

3. Consolute point line within the magnetic phase, a tricritical plait point line with two tricritical end points, and a plait point line

Even more critical points may exist at the same pressure. This happens for the case of mixing a van der Waals fluid with a slightly different (smaller strength of magnetic interaction) Ising fluid. For the parameters $\zeta=0.5$, $\Lambda=-0.12$, and $R_m=0.2$, it is even possible to have two tricritical plait

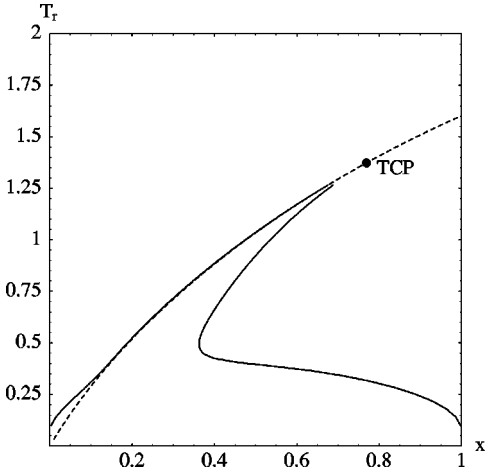

FIG. 14. x, T_r diagram of a mixture with $\zeta=0.5$, $\Lambda=-0.25$, and $R_m=0.5$ at $p_r=5.5$. TCP, tricritical point; full lines, first-order phase transitions; dashed line, magnetic phase transitions.

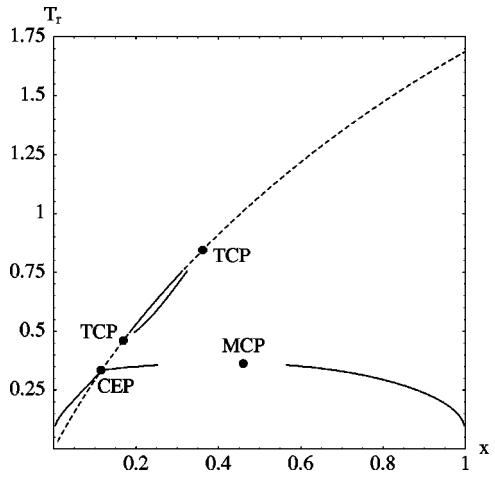

FIG. 15. x, T_r diagram of a mixture with $\zeta=0.5$, $\Lambda=-0.25$, and $R_m=0.5$ at $p_r=6.75$. TCP, tricritical point; MCP, magnetic consolute point; CEP, critical end point; full lines, first-order phase transitions; dashed line, magnetic phase transitions.

points, a plait point, and a consolute point in the magnetic phase at the same pressure (see Fig. 18).

The corresponding three-dimensional phase diagram (Fig. 19) shows a tricritical line that separates the surface of second-order magnetic phase transitions from first-order liquid phase transitions. No tricritical point is present at $x=1$ and $x=0$; instead, the tricritical line bends over from one tricritical end point to another one at lower concentration. One of these tricritical end points lies on the gas liquid first-order phase transition surface, the other one on the first-order demixing phase transition surface. Demixing takes place in the ferromagnetic phase as in the example mentioned before.

VIII. DISCUSSION

We have investigated mixtures of a van der Waals fluid and an Ising fluid and have found that besides the usual

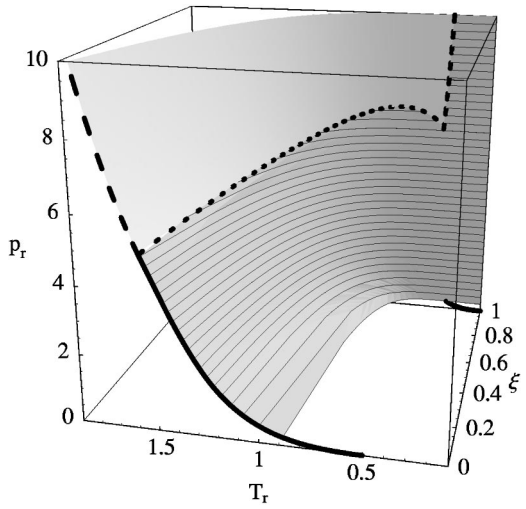

FIG. 16. ξ, T_r, p_r diagram of a mixture with $\zeta=0.5$, $\Lambda=-0.25$, and $R_m=0.5$. Thick lines, liquid-vapor curves of the pure substances; thin lines, isobaric curves on the first-order surface; dotted line, tricritical line; dashed lines, critical lines.

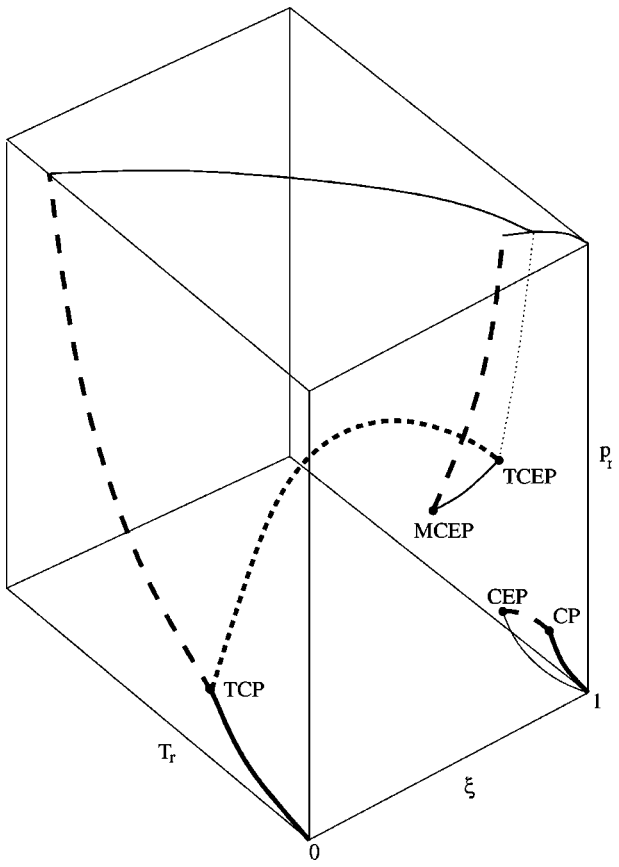

FIG. 17. Schematic ξ, T_r, p_r diagram of a mixture with $\zeta=0.5$, $\Lambda=-0.25$, and $R_m=0.5$, the region near $\xi=1$ is magnified. Thick lines, liquid-vapor curves of the pure substances; thin lines, lines of triple points; thick dotted line, tricritical line; thin dotted line, line of critical end points; dashed lines, lines of critical points; TCP, tricritical point; MCEP, magnetic critical end point; TCEP, tricritical end point; CP, critical point; CEP, critical end point.

critical lines and coexistence surfaces such systems exhibit magnetic critical lines and tricritical lines, whose existence and shape depend on the three mixture parameters ζ, Λ, and R_m. The tricritical line can either have the character of a consolute line and continue until infinite pressure, or it stays at finite pressure and ends on a coexistence surface. In this case it has the character of a plait point line. Moreover, there is still immiscibility at higher pressures, and a line of magnetic consolute points extends to infinite pressure.

These findings within the mean field theory will be corroborated by further investigations using Gibbs ensemble Monte Carlo simulations [27,28]. Fluctuation effects are expected to change shape and location of transition lines and surfaces. Both magnetic and liquid phase transitions show critical exponents different from mean field exponents. This has also been proven for the magnetic liquid [29].

ACKNOWLEDGMENT

We acknowledge support by the Fonds zur Förderung der wissenschaftlichen Forschung under Project No. P15247-TPH.

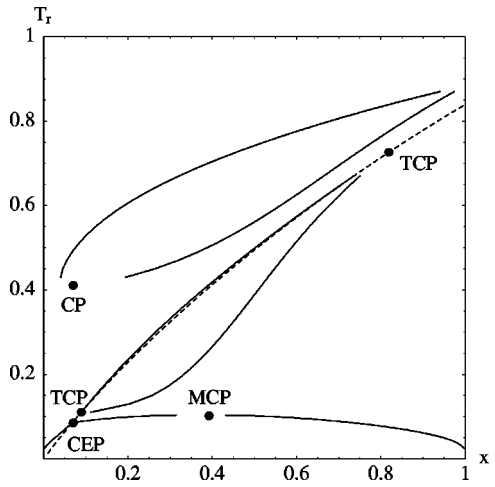

FIG. 18. x, T_r diagram of a mixture with $\zeta=0.5$, $\Lambda=-0.12$, and $R_m=0.2$ at $p_r=0.6$. CP, critical point; TCP, tricritical point; MCP, magnetic consolute point; CEP, critical end point; full lines, first-order phase transitions; dashed line, magnetic phase transitions.

APPENDIX A: REPRESENTATION OF THE PHASE DIAGRAMS

We present the phase diagrams of the magnetic liquid mixtures in two ways. First we show the phase diagram in the space of the usual physical thermodynamic variables, which are pressure, temperature, and concentration. Since the concentration is a density and not a field, the character of the demixing transitions is seen as a multivalued surface of the two fields. These diagrams are accompanied with the usual two-dimensional constant pressure sections. In fact, the stack of these sections builds up the three-dimensional diagrams.

If we choose all three thermodynamic fields as variables the different phases are separated by single valued surfaces in the thermodynamic field space. This illustrates, in our opinion, the overall picture of the different phases more clearly and seems to be appropriate for theoretical considerations in the sense of Griffith and Wheeler [30]. These surfaces join together in special lines, which might be lines of triple points in the case first-order transition surfaces meet. In the case where a first-order transition surface meets a surface of second-order transitions we find either lines of critical end points or lines of tricritical points if it happens that the surface of second-order phase transitions meets the coexistence surface in the border line of critical points.

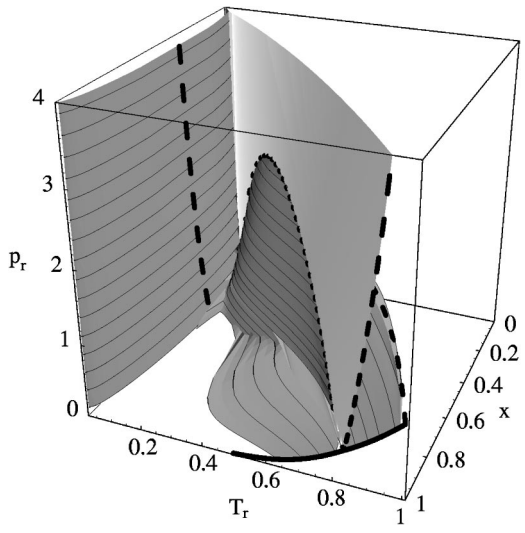

FIG. 19. x, T_r, p_r diagram of a mixture with $\zeta=0.5$, $\Lambda=-0.12$, and $R_m=0.2$. Thick lines, liquid-vapor curves of the pure substances; thin lines, isobaric curves on the first-order surface; dotted line, tricritical line; dashed lines, critical lines.

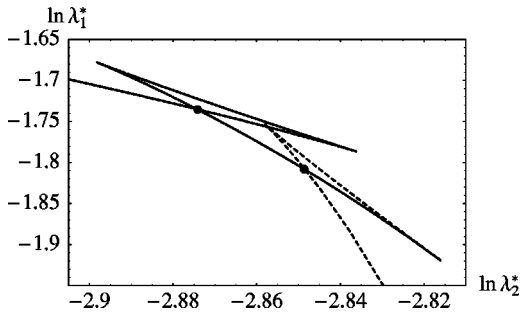

FIG. 20. Plot of the curve $[\ln\lambda_1^*(V_r),\ln\lambda_2^*(V_r)]$ for $\zeta=0.5$, $\Lambda=-0.05$, $R_m=0.2$, $p_r=0.9$, $T_r=0.8$. Along the dashed part of the curve the magnetization is finite. The self-intersection points are indicated with dots.

APPENDIX B: MAGNETIC CRITICAL LINES

In the following equations we make use of the dimensionless quantities:

$$\overline{T}\equiv\frac{4}{27R_m}T_r, \tag{B1}$$

$$y\equiv(1-m^2)^{-1}, \tag{B2}$$

$$\alpha\equiv\left(\frac{1}{R_m}+m^2\right)x^2+\frac{2}{R_m}\frac{1-\Lambda}{1+\zeta}x(1-x)+\frac{1}{R_m}\frac{1-\zeta}{1+\zeta}(1-x)^2, \tag{B3}$$

$$\beta\equiv\frac{1}{2}\frac{d\alpha}{dx}, \tag{B4}$$

$$\gamma\equiv\frac{d\beta}{dx}, \tag{B5}$$

$$\eta\equiv\frac{\overline{T}}{2}[\ln(1+m)-\ln(1-m)]-\frac{2xm}{V_r}, \tag{B6}$$

$$\varepsilon\equiv V_r\overline{T}-x(1-m^2), \tag{B7}$$

$$u\equiv(2-6m^2+4m^4)\varepsilon-2x(1-m^2)^2m^2, \tag{B8}$$

$$z\equiv x(1-x), \tag{B9}$$

$$w\equiv 1-2x. \tag{B10}$$

The derivatives of the magnetization with respect to the concentration are then given by

$$m_x=\frac{1}{\varepsilon}(1-m^2)m, \tag{B11}$$

$$m_{2x}=\frac{mu}{\varepsilon^3}. \tag{B12}$$

Now Eq. (20) with finite magnetization yields

$$F_1(\overline{T},V_r,x,m)\equiv[(V_r-1)^2(\alpha+x^3mm_x)-V_r^3\overline{T}]\times[\gamma z-V_r\overline{T}-zV_r\eta m_x]-(\beta-xV_r\eta m_x)^2z\times(V_r-1)^2=0, \tag{B13}$$

and from Eq. (21) we obtain

$$F_2(\overline{T},V_r,x,m)\equiv[\{3\alpha+x^3[6mm_x+x(m_x^2+mm_{2x})]\}(V_r-1)^3-2\overline{T}V_r^4][z(\gamma-V_r\eta m_x)-\overline{T}V_r]^2-3z\{2\beta+x^2\times[5mm_x+x(m_x^2+mm_{2x})]\}(\beta-V_rx\eta m_x)[z(\gamma-V_r\eta m_x)-\overline{T}V_r](V_r-1)^3+3z^2\{\gamma+x[4mm_x-(\overline{T}V_ry-2x)\times m_x^2-V_r\eta m_{2x}]-V_r\eta m_x\}(\beta-V_rx\eta m_x)^2(V_r-1)^3-\{\overline{T}V_rw-z^2[V_r\eta m_{2x}-4mm_x+(\overline{T}V_ry-2x)m_x^2]\}\times[(\alpha+x^3mm_x)(V_r-1)^2-\overline{T}V_r^3](\beta-V_rx\eta m_x)(V_r-1)=0. \tag{B14}$$

At a particular pressure p_0, a critical point in the ferromagnetic phase can be found by solving the four equations

$$F_1(\overline{T},V_r,x,m)=0, \tag{B15}$$

$$F_2(\overline{T},V_r,x,m)=0, \tag{B16}$$

$$m=\tanh\left(\frac{xm}{V_r\overline{T}}\right), \tag{B17}$$

$$p_r(\overline{T},V_r,x,m)=p_0, \tag{B18}$$

for the variables $\overline{T}$, V_r, x, m. Only the thermodynamic equation of state (B18) can be solved analytically for x, the other equations have to be solved numerically, which requires appropriate starting values for $\overline{T}$, V_r, and m to be known.

The numerical function that was applied to solve Eqs. (B15)–(B17) uses a modification of the Powell hybrid method for nonlinear algebraic equations [31].

APPENDIX C: TRICRITICAL LINE

The equation for the tricritical line is obtained from Eq. (B13) when the magnetization tends to zero and T approaches the critical temperature of the magnetic phase transition given by Eq. (25), which is

$$\overline{T}_c=\frac{x}{V_r} \tag{C1}$$

in reduced quantities. For the term mm_x, we have

$$\lim_{\substack{m\to0\\ \overline{T}\to\overline{T}_c}} mm_x=\lim_{\substack{m\to0\\ \overline{T}\to\overline{T}_c}}\frac{m^2}{V_r\overline{T}-x(1-m^2)}. \tag{C2}$$

Substituting m^2 with the expansion of the magnetic equation of state,

$$m^2\sim3\left(1-\frac{V_r\overline{T}}{x}\right), \tag{C3}$$

we get as a result

$$\lim_{\substack{m\to0\\ \overline{T}\to\overline{T}_c}} mm_x=\frac{3}{2x}. \tag{C4}$$

Similarly, we obtain for ηm_x,

$$\lim_{\substack{m\to0\\ \overline{T}\to\overline{T}_c}} \eta m_x=\lim_{\substack{m\to0\\ \overline{T}\to\overline{T}_c}}\left(\frac{\overline{T}}{2}[\ln(1+m)-\ln(1-m)]-\frac{2xm}{V_r}\right)m_x=\left(\overline{T}_c-\frac{2x}{V_r}\right)\lim_{\substack{m\to0\\ \overline{T}\to\overline{T}_c}} mm_x=-\frac{3\overline{T}_c}{2x}. \tag{C5}$$

Substituting Eqs. (C4) and (C5) into Eq. (B13) and replacing the volume with the critical volume from Eq. (25) leads to Eq. (29) for the tricritical temperature.

APPENDIX D: PHASE EQUILIBRIA

Phase equilibria were calculated from Eqs. (12) and (13), where the dimensionless relative activity λ_i^*, defined as

$$\ln\lambda_i^*=\frac{\mu_i^{rel}}{RT},\quad i=1,2, \tag{D1}$$

was used instead of the relative chemical potentials. This was done by solving Eq. (16), which is quadratic in x, and substituting the solution $x_i(V_i,m_i)$ into Eqs. (12) and (13) and

Eq. (17). Finding the solution to Eqs. (12) and (13) is then equivalent to finding a self-intersection point of a curve in the $\ln\lambda_1^*$, $\ln\lambda_2^*$ plane, parametrized by the volume V_r. Along this curve, the magnetization varies as a function of V_r according to Eq. (17) between 0 and 1. Figure 20 shows an example of such a curve with two self-intersections corresponding to a nonmagnetic gas-liquid and a paramagnetic-ferromagnetic liquid-liquid phase transition. Equations (12) and (13) were again solved via the Powell hybrid method [31].

[1] P.H. van Konynenburg and R.L. Scott, Philos. Trans. R. Soc. London, Ser. A **298**, 495 (1980).
[2] L.Z. Boshkov, Dokl. Akad. Nauk SSSR **294**, 901 (1987).
[3] A. van Pelt, C.J. Peters, and J. de Swaan Arons, J. Chem. Phys. **95**, 7569 (1991).
[4] A. van Pelt and T.W. de Loos, J. Chem. Phys. **97**, 1271 (1992).
[5] D. Furman, S. Dattagupta, and R.B. Griffiths, Phys. Rev. B **15**, 441 (1977).
[6] D. Furman and R.B. Griffiths, Phys. Rev. A **17**, 1139 (1978).
[7] M. Keskin, M. Gençaslan, and P.H.E. Meijer, J. Stat. Phys. **66**, 885 (1992).
[8] M. Gençaslan and M. Keskin, Physica A **293**, 28 (2001).
[9] U.K. Deiters and I.L. Pegg, J. Chem. Phys. **90**, 6632 (1989).
[10] T. Kraska and U.K. Deiters, J. Chem. Phys. **96**, 539 (1992).
[11] N.B. Wilding, F. Schmid, and P. Nielaba, Phys. Rev. E **58**, 2201 (1998).
[12] E. Schöll-Paschinger, D. Levesque, J.-J. Weis, and G. Kahl, Phys. Rev. E **64**, 011502 (2001).
[13] P.H.E. Meijer, M. Keskin, and I.L. Pegg, J. Chem. Phys. **88**, 1976 (1988).
[14] C.M. Knobler and R.L. Scott, in *Phase Transitions and Critical Phenomena*, edited by C. Domb and J.L. Lebowitz (Academic Press, London, 1984), Vol. 9, p. 163.
[15] P.C. Hemmer and D. Imbro, Phys. Rev. A **16**, 380 (1977).
[16] J.M. Tavares, M.M.T. da Gama, P.I.C. Teixeira, J.-J. Weis, and M.J.P. Nijmeijer, Phys. Rev. E **52**, 1915 (1995).
[17] J.M. Tavares, P.I.C. Teixeira, and M.M.T. da Gama, Phys. Rev. E **58**, 3175 (1998).
[18] A. Oukouiss and M. Baus, Phys. Rev. E **55**, 7242 (1997).
[19] J. Reske, D.M. Herlach, F. Keuser, K. Maier, and D. Platzek, Phys. Rev. Lett. **75**, 737 (1995).
[20] T. Albrecht, C. Bührer, M. Fähnle, K. Maier, D. Platzek, and J. Reske, Appl. Phys. A: Mater. Sci. Process. **65**, 215 (1997).
[21] E. Lomba, J.-J. Weis, N.G. Almarza, F. Bresme, and G. Stell, Phys. Rev. E **49**, 5169 (1994).
[22] J.-J. Weis, M.J.P. Nijmeijer, J.M. Tavares, and M.M.T. da Gama, Phys. Rev. E **55**, 436 (1997).
[23] M.J.P. Nijmeijer, A. Parola, and L. Reatto, Phys. Rev. E **57**, 465 (1998).
[24] J.W. Essam, in *Phase Transitions and Critical Phenomena*, edited by C. Domb and M.S. Green (Academic Press, London, 1972), Vol. 2.
[25] G. Schneider, Ber. Bunsenges. Phys. Chem. **70**, 497 (1966).
[26] G. Schneider, Ber. Bunsenges. Phys. Chem. **76**, 325 (1972).
[27] A.Z. Panagiotopoulos, Mol. Phys. **61**, 813 (1987).
[28] A.Z. Panagiotopoulos, N. Quirke, M. Stapleton, and D.J. Tildesley, Mol. Phys. **63**, 527 (1988).
[29] C. Bührer, M. Beckmann, M. Fähnle, U. Grünewald, and K. Maier, J. Magn. Magn. Mater. **212**, 211 (2000).
[30] R.B. Griffiths and J.C. Wheeler, Phys. Rev. A **2**, 1047 (1970).
[31] M.J.D. Powell, in *Numerical Methods for Nonlinear Algebraic Equations*, edited by P. Rabinowitz (Gordon and Breach, New York, 1970).